Science Advances
AAAS

Supplementary Materials for

Development of iPSC-based clinical trial selection platform for patients with ultrarare diseases

Glen Lester Sequiera, Abhay Srivastava, Niketa Sareen, Weiang Yan, Keshav Narayan Alagarsamy, Elika Verma, Mohamad Reza Aghanoori, Michel Aliani, Ashok Kumar, Paul Fernyhough, Cheryl Rockman-Greenberg, Sanjiv Dhingra*

*Corresponding author. Email: sdhingra@sbrc.ca

Published 8 April 2022, *Sci. Adv.* **8**, eabl4370 (2022)
DOI: 10.1126/sciadv.abl4370

This PDF file includes:

Figs. S1 to S22
Table S1

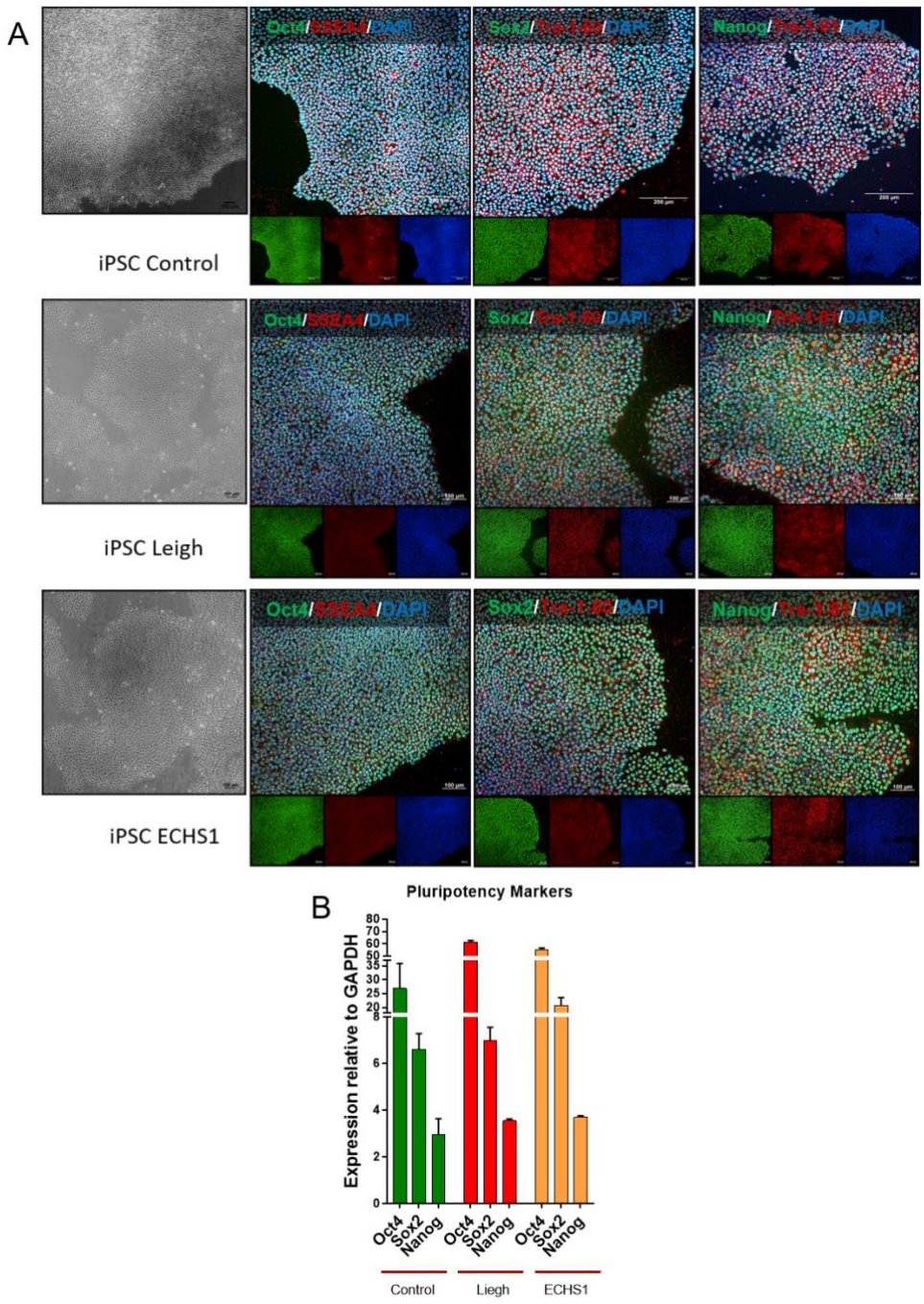

Supplementary Figure S1. Characterization of iPSC. **A** PBMCs extracted from blood were reprogrammed to iPSC using Sendai virus reprogramming kit. To characterize iPSC, the cells were immunostained with pluripotency markers – Oct4/ SSEA4, Sox2/ Tra-1-60 and Nanog/Tra-1-81 (scale bars =100 µm for ECHS1 and LS iPSC; 200 µm for control iPSC) (n=3). Oct4, Sox2 and Nanog are green and SSEA4, Tra-1-60 and Tra-1-80 are red. Nucleus was stained with DAPI (blue). **B** The pluripotency was further confirmed by real time PCR analysis for Oct4, Sox2 and Nanog transcript expression relative to GAPDH in control, LS and ECHS1 patient cell lines. The data is representative of three independent experiments.

Sample	Sex	Status
Control Female 1	Female	Normal
Control Female 2	Female	Normal
Control Male 1	Male	Normal (Sex Difference)
Control Male 2	Male	Normal (Sex Difference)
LS (Leigh)	Female	Normal
SCEH (ECHS1)	Male	Normal (Sex Difference)

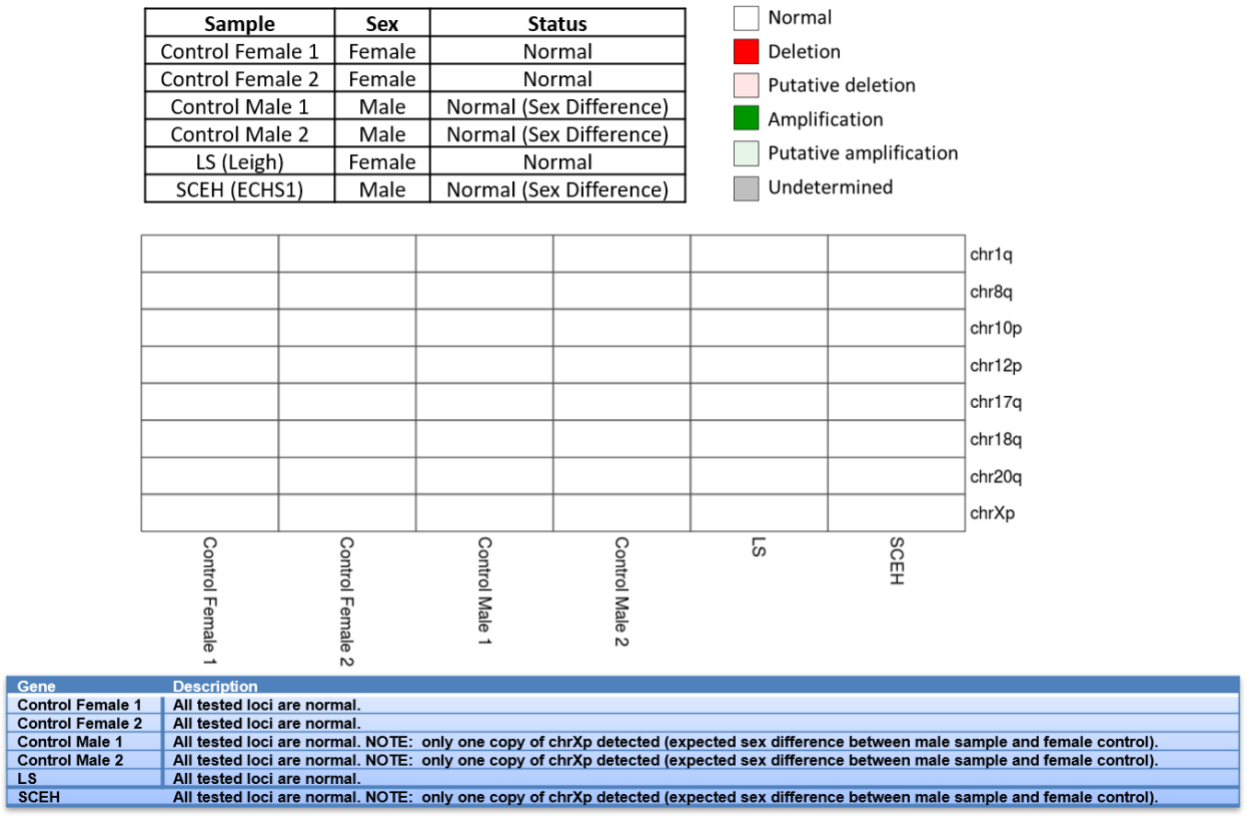

Gene	Description
Control Female 1	All tested loci are normal.
Control Female 2	All tested loci are normal.
Control Male 1	All tested loci are normal. NOTE: only one copy of chrXp detected (expected sex difference between male sample and female control).
Control Male 2	All tested loci are normal. NOTE: only one copy of chrXp detected (expected sex difference between male sample and female control).
LS	All tested loci are normal.
SCEH	All tested loci are normal. NOTE: only one copy of chrXp detected (expected sex difference between male sample and female control).

Supplementary Figure S2. Characterization of iPSC- chromosome aberration analyses: The karyotypic abnormalities over the course of passaging are frequently reported *in vitro* cultures. qPCR was performed to investigate the presence of karyotypic abnormalities in iPSC at intervals of 20-25 passages. None of the cell lines generated in the study reported any karyotypic abnormalities at the time of differentiation and subsequent experimentation (n=3). The data are representative of three independent experiments.

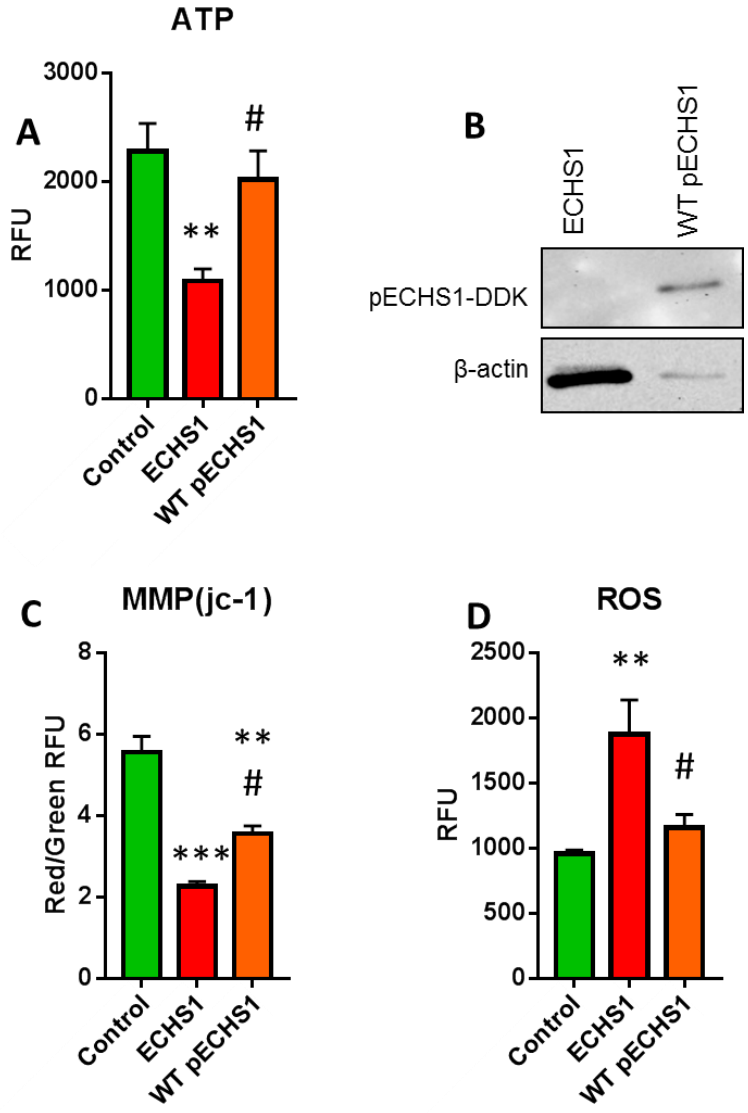

Supplementary Figure S3. Expressing WT pECHS1 in iPSC derived fibroblasts of ECHS1 patient improves mitochondrial bioenergetics: A ATP levels increased significantly in cells transfected with ECHS1 expression vector. compared to diseased fibroblasts (n=8-10). **B** Immunoblot for ECHS1 tagged with DDK confirmed transfection and expression of wild type ECHS1 in diseased fibroblasts (n=3)**. C** Mitochondrial membrane potential analysis showed a significant increase in Ψm in transfected cells compared to diseased fibroblasts (n=8-10). **D** Total ROS analysis showed a significant decrease in ROS in transfected cells compared to diseased fibroblasts (n=8-10). The "n" is representative of the biological replicates and were analyzed by one-way ANOVA. The data are representative of three independent experiments. Data are presented as mean ± SEM; * $p<0.05$; ** $p<0.01$ and *** $p<0.001$ in comparison to control; # $p<0.05$ and ## $p<0.01$ against ECHS1.

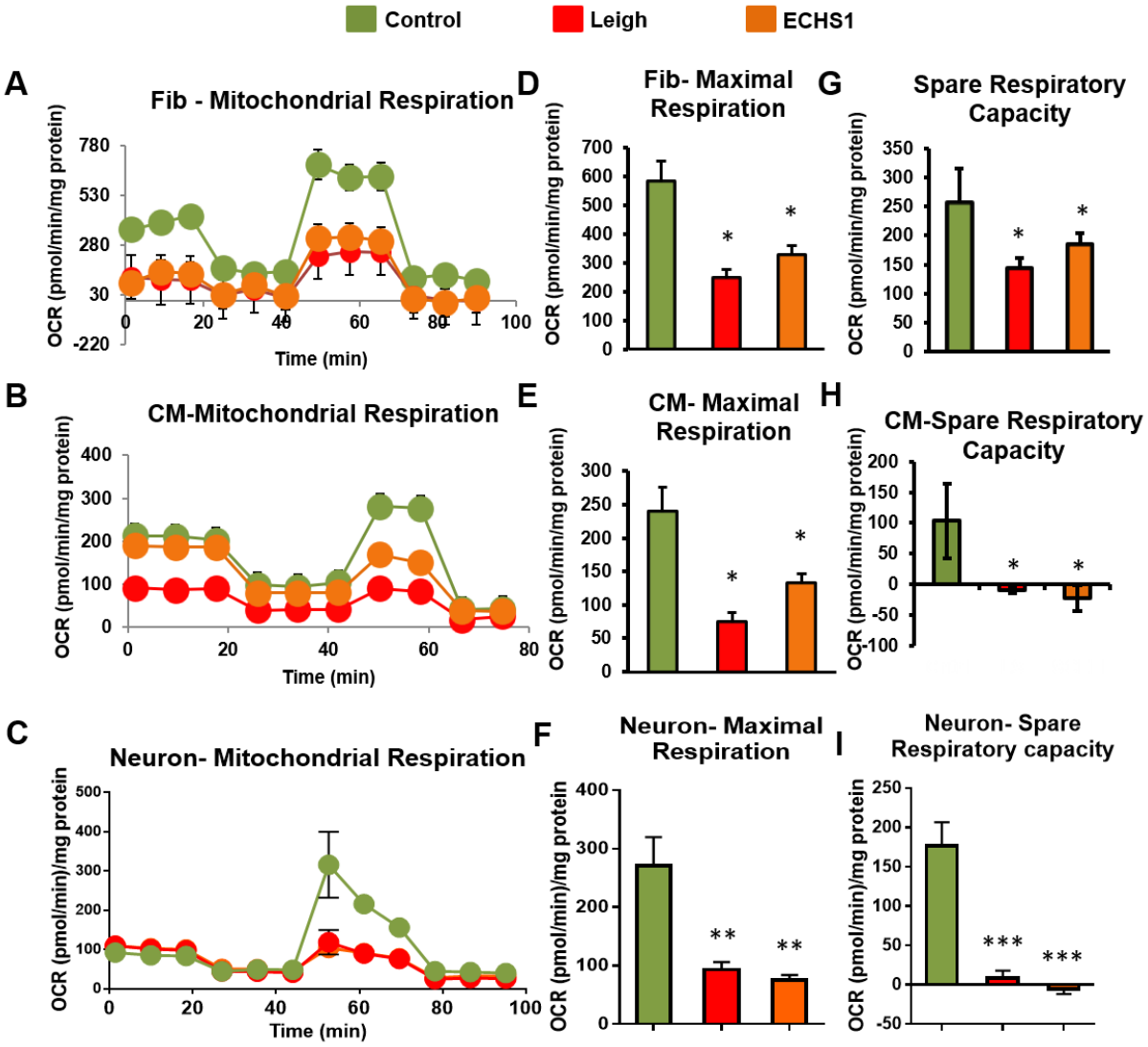

Supplementary Figure S4. Cellular bioenergetics and mitochondrial respiration analyses: A-C Mitochondrial respiration in fibroblasts, CMs and neurons as carried out using SeaHorse XFe24 analyser was adversely affected in the patient cells compared to healthy control; **D-F** Maximal respiration decreased significantly in patient fibroblasts, CMs and neurons compared to healthy control cells; **G-I** Spare respiratory capacity downregulated significantly in patient fibroblasts, CMs and neurons compared to healthy control cells. These parameters are strong indicators for mitochondrial dysfunction, providing evidence for compromised cellular respiration kinetics in patients' cells compared to healthy control cells. The "n" is representative of the biological replicates and were analyzed by one-way ANOVA. The data are representative of three independent experiments. Data are represented as mean ± SEM; *p<0.05 **p<0.01 and ***p<0.001 in comparison to control.

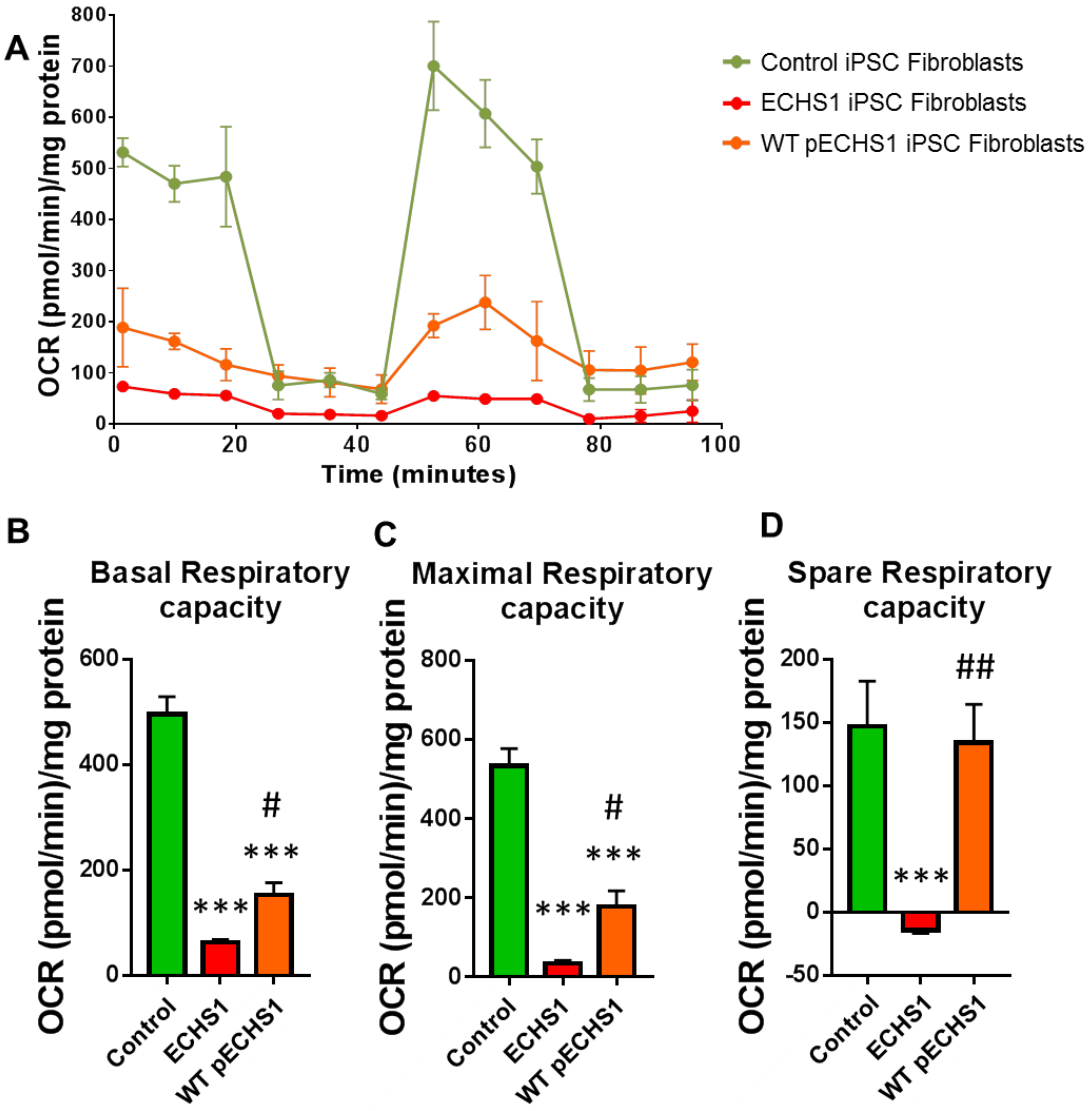

Supplementary Figure S5. Expressing WT pECHS1 in iPSC derived fibroblasts of ECHS1 patient improved mitochondrial bioenergetics: A-D Mitochondrial respiration (A), basal respiratory capacity (B), maximal respiratory capacity (C) and spare respiratory capacity (D) in Control, ECHS1 and WT pECHS1 expressed fibroblasts was carried out using SeaHorse XFe24 analyser (n=4). There was a significant decrease observed in these parameters in ECHS1 fibroblasts compared to healthy control cells, however maintaining ECHS1 protein levels using expression vector led to significant improvement in all these parameters. The "n" is representative of the biological replicates and were analyzed by one-way ANOVA. The data are representative of three independent experiments. Data are represented as mean ± SEM; *p<0.05 **p<0.01 and ***p<0.001 in comparison to control; #p<0.05 ##p<0.01 and ###p<0.001 in comparison to ECHS1.

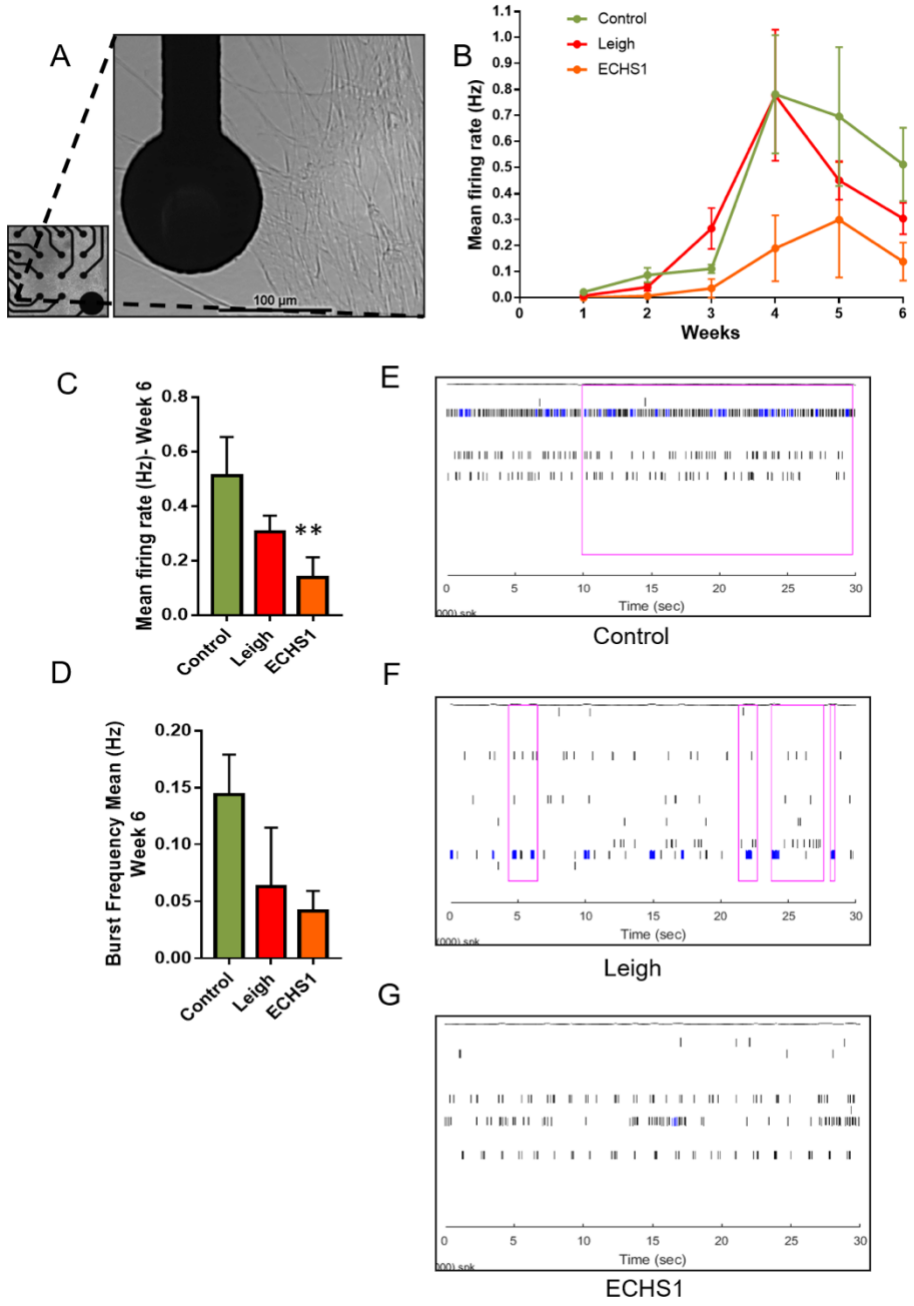

Supplementary Figure S6. MEA analysis of iPSC derived neurons: A Neurons cultured on MEA plate with micro electrodes (n=6-8, scale bar 100 µm). **B** To assess neuronal activity, mean firing rate in control, Leigh and ECHS1 neurons was compared for a period of 6 weeks of neuronal maturation (n=6-8). **C** Mean firing rate at 6 weeks of neuronal maturation (n=6-8). **D** Burst frequency mean at 6 weeks of neuronal maturation (n=6-8). **E-G** Raster plots showing spikes and bursts to display neuronal activity in control, Leigh and ECHS1 iPSC derived neurons. Each line is a spike recorded by firing of neurons and 5 continuous spikes make up a single burst, which is represented by a blue line. A series of bursts from neighbouring neurons make up a network burst

represented by the activity in the purple box (n=6-8). The "n" is representative of the biological replicates and were analyzed by one-way ANOVA. The data are representative of three independent experiments and presented as mean ± SEM; *p<0.05 **p<0.01 and ***p<0.001 in comparison to control.

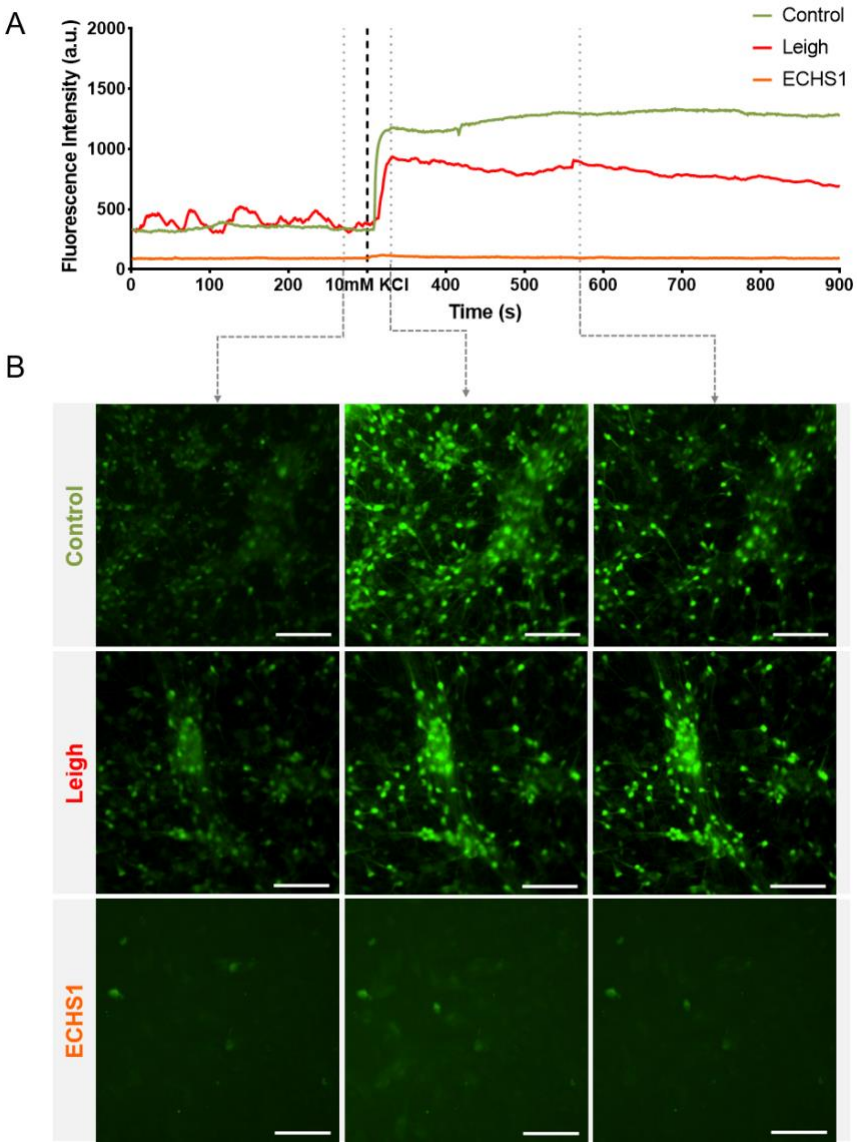

Supplementary Figure S7. Assessment of calcium handling in iPSC derived neurons: A Assessment of calcium handling in control, Leigh and ECHS1 iPSC neurons when evoked with 10mM KCl (n=3). **B** Images depicting calcium response at pre, just after evoking and during decay of calcium transits in control, Leigh and ECHS1 neurons (n=3). The "n" is representative of the biological replicates. The scale bar is 100 µm.

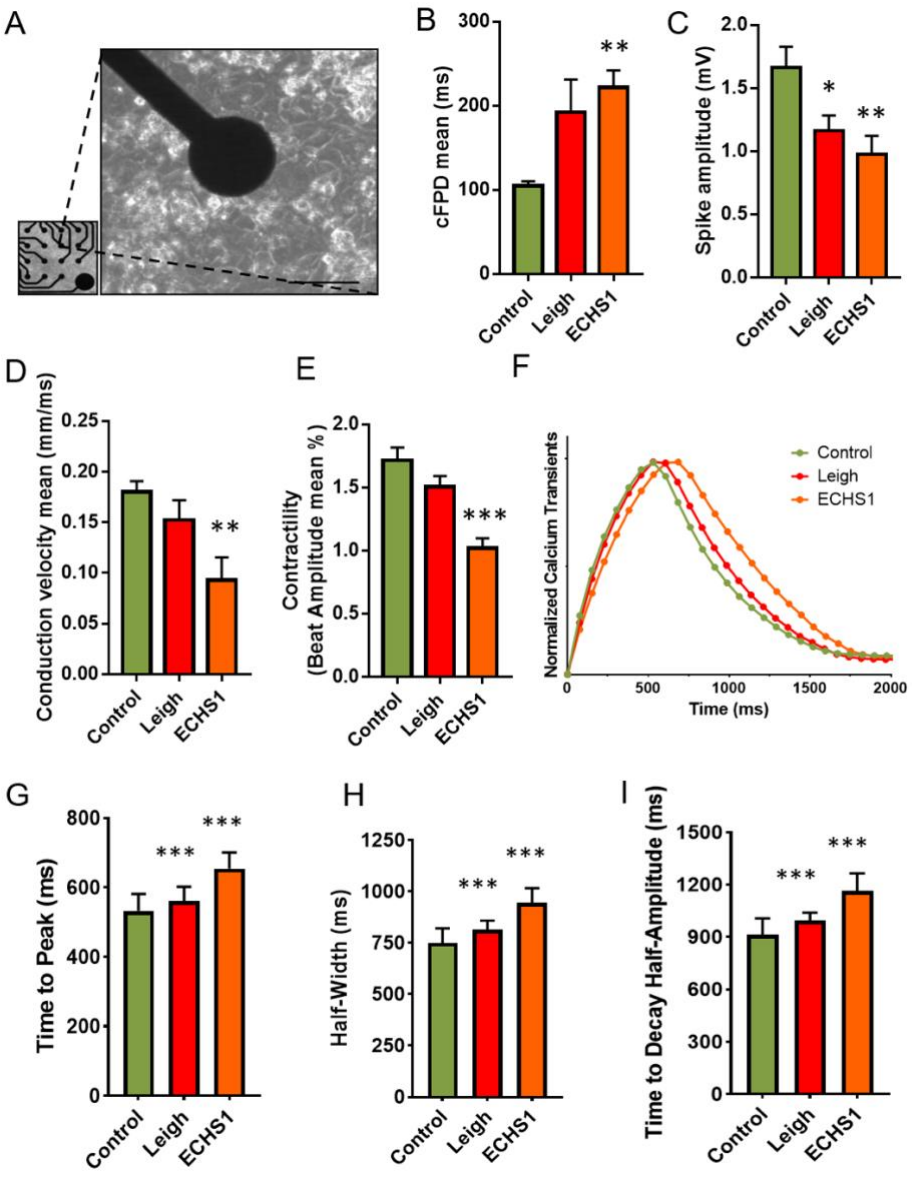

Supplementary Figure S8. MEA analysis and calcium handling assessment of iPSC derived cardiomyocytes: A Cardiomyocytes cultured on MEA plate with micro electrodes (scale bar 100 µm) **B-E** Histograms showing corrected field potential delay, spike amplitude, conduction velocity and contractility in control, Leigh and ECHS1 iPSC-CMs (n=6). **F** Normalized action potential calcium transits in control, Leigh and ECHS1 iPSC-CMs (n=10). **G-I** Action potential wave properties of time to peak, half-width and time to decay half-amplitude in control, Leigh and ECHS1 CMs. Data were collected from 10 different regions of interest per loop and 80-130 beats were analyzed and plotted for every group of CMs. The "n" is representative of the biological replicates and were analyzed by one-way ANOVA. The data are representative of three independent experiments and presented as mean ± SEM; * $p<0.05$; **$p<0.01$ and ***$p<0.001$ in comparison to control.

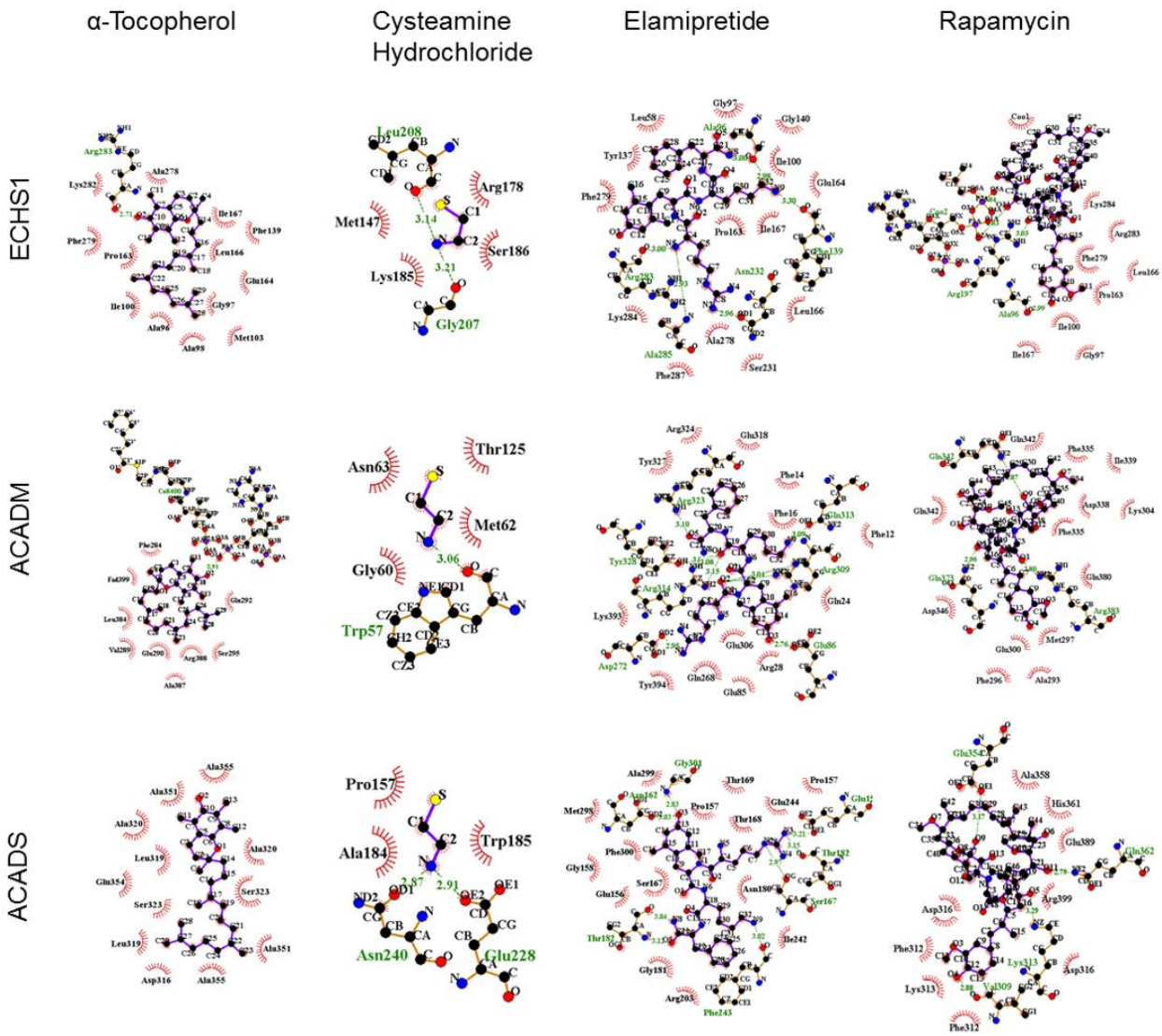

Supplementary Figure S9. Evaluation of drug interactions with ECHS1 and related enzymes: In silico analysis was performed to assess the interaction of α-tocopherol (Toco), cysteamine hydrochloride (Cys), rapamycin (Rapa) and elamipretide (Elam) with ECHS1, ACADM (Medium-chain specific acyl-CoA dehydrogenase, mitochondrial) and ACADS (Short-chain specific acyl-CoA dehydrogenase, mitochondrial). These enzymes are reported to downregulate the accumulation of derogatory by-products in ECHS1 patients. The figure depicts molecular interaction of Toco, Cys, Elam and Rapa with ECHS1, ACADM and ACADS respectively using docking analysis. This analysis depicts top docking site/pockets where the drug interacted with respective target molecules and their molecular binding sites.

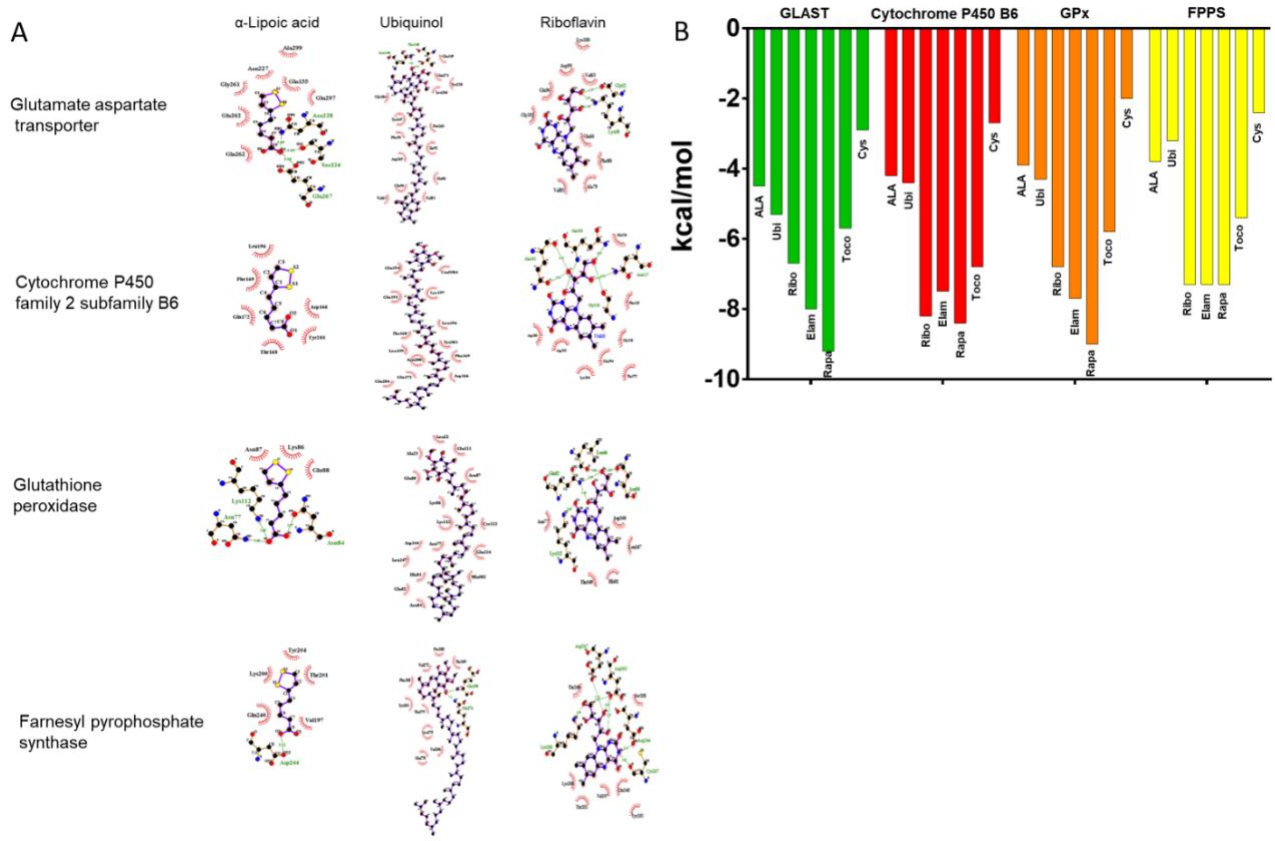

Supplementary Figure S10. Evaluation of drug interactions with Targets involved in regulating energy flux and ROS: A In silico analysis to assess the interaction of Ubiquinol (Ubi), α-lipoic acid (ALA) and Riboflavin (Ribo) with targets affecting energy metabolism such as glutamate aspartate transporter (GLAST) and cytochrome P450 family 2 subunit B6 family protein along with targets regulating ROS such as glutathione peroxidase (GPx) and farnesyl pyrophosphate synthase (FPPS). Here the top docking site/pockets are shown where the drug interacted with respective target molecules to understand multitudinous interactions among drugs and their molecular binding sites using LigPlus software. **B** Histograms depict respective molecular docking analysis that show favourable binding energy for interactions between Ubi, ALA, Ribo, Toco, Cys, Rapa and Elam with GLAST and Cytochrome P450 family 2 subunit B6 family protein, GPx and FPPS. Furthermore, to evaluate the protein-ligand binding at the molecular level the binding energy was expressed in terms of kcal/mol (kilocalorie per mole). 'kcal/mol' defines the energy density (binding energy) of the interaction between the two molecules in question. The stability of an interaction is inversely proportional to their binding energy, which is represented here. Hence, the figure shows a direct relationship between more negative binding energy and the probability of increased stable interaction among the drug and respective ligands.

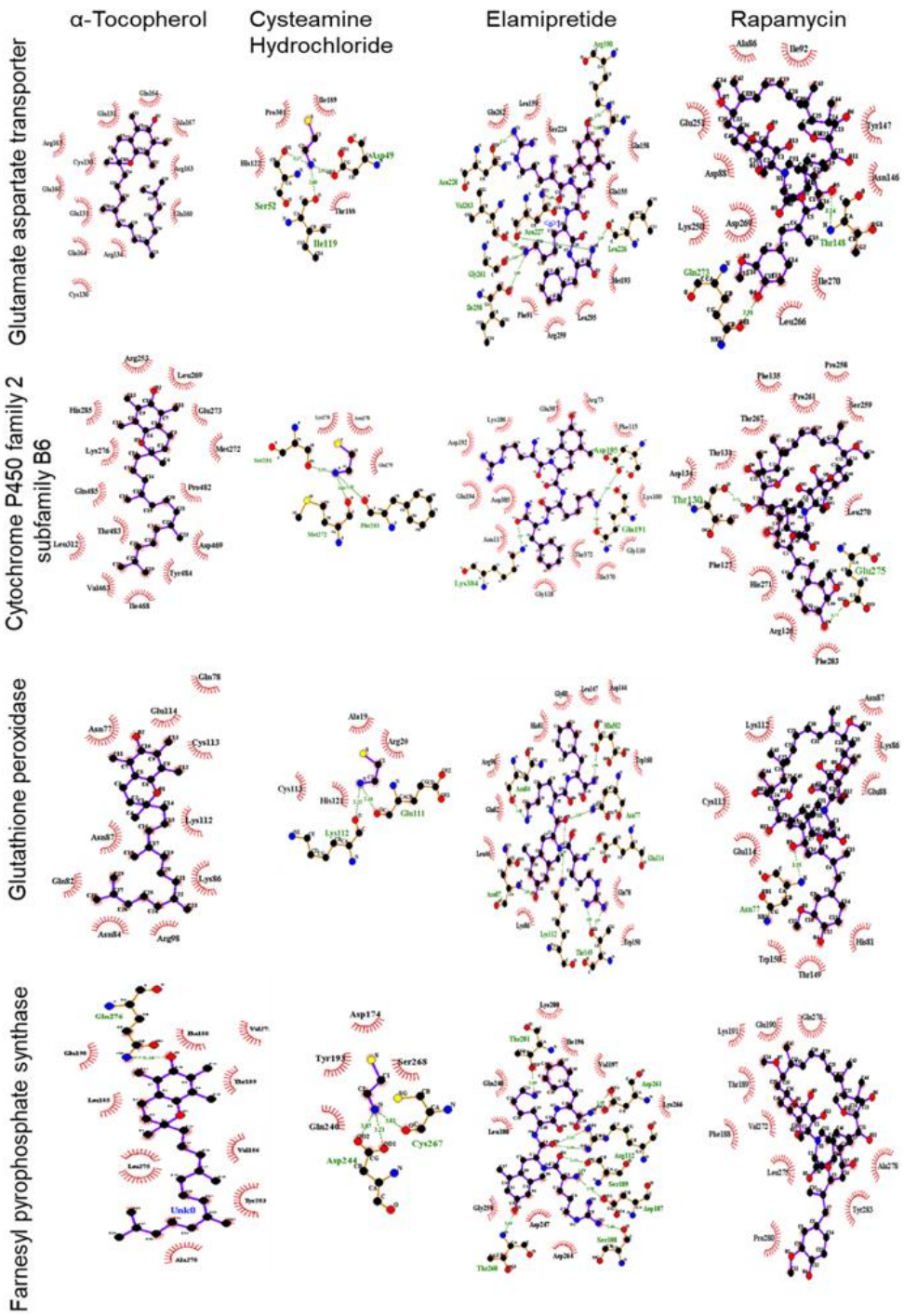

Supplementary Figure S11. Evaluation of drug interactions with targets involved in regulating energy flux and ROS. In silico analysis to assess the interaction of α-tocopherol (Toco), Cysteamine hydrochloride (Cys), Elamipretide (Elam) and Rapamycin (Rapa) with targets affecting energy metabolism such as glutamate aspartate transporter (GLAST) and cytochrome P450 family 2 subunit B6 family protein along with targets regulating ROS such as glutathione

peroxidase (GPx) and farnesyl pyrophosphate synthase (FPPS). Here we show visualization of the top docking site/pockets where the drug interacted with respective target molecules to understand multitudinous interactions among drugs and their molecular binding sites using LigPlus software.

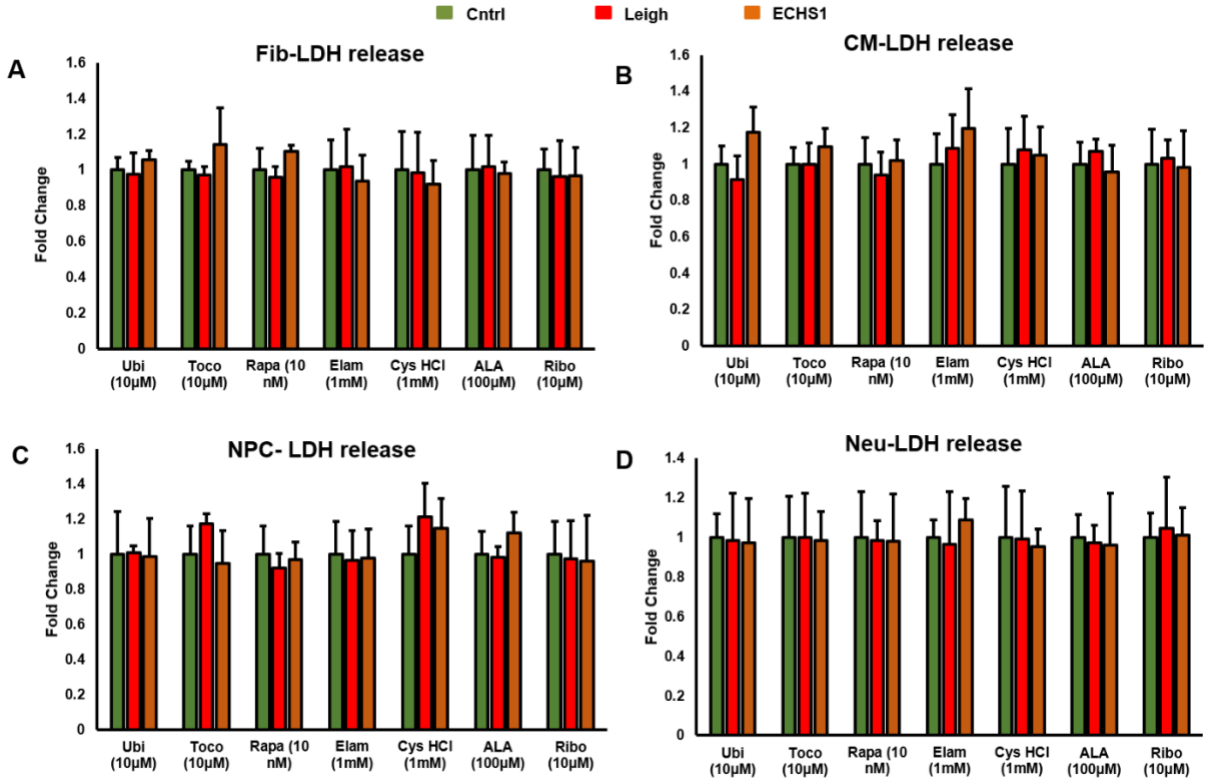

Supplementary Figure S12. Assessment of safety of drug panel: Safety of a panel of seven drugs- Coenzyme Q10 (Ubiquinol: Ubi), Alpha-lipoic acid (ALA), Alpha-tocopherol (Toco), Cysteamine hydrochloride (Cys), Rapamycin (Rapa), Elamipretide (Elam) and Riboflavin (Ribo) was evaluated by assessing the level of toxicity (LDH release) caused by individual drugs in different cells- fibroblasts, NPCs, CMs and neurons. **A** Toxicity analysis through LDH release in fibroblasts (n=5). **B** Toxicity analysis through LDH release in CMs (n=5). **C** Toxicity analysis through LDH release in NPCs (n=5). **D** Toxicity analysis through LDH release in neurons (n=5). None of the drugs showed any cytotoxicity at the concentrations tested in the study. The "n" is representative of the biological replicates and were analysed by unpaired t test. The data is representative of three independent experiments. Data is represented as mean ± SD.

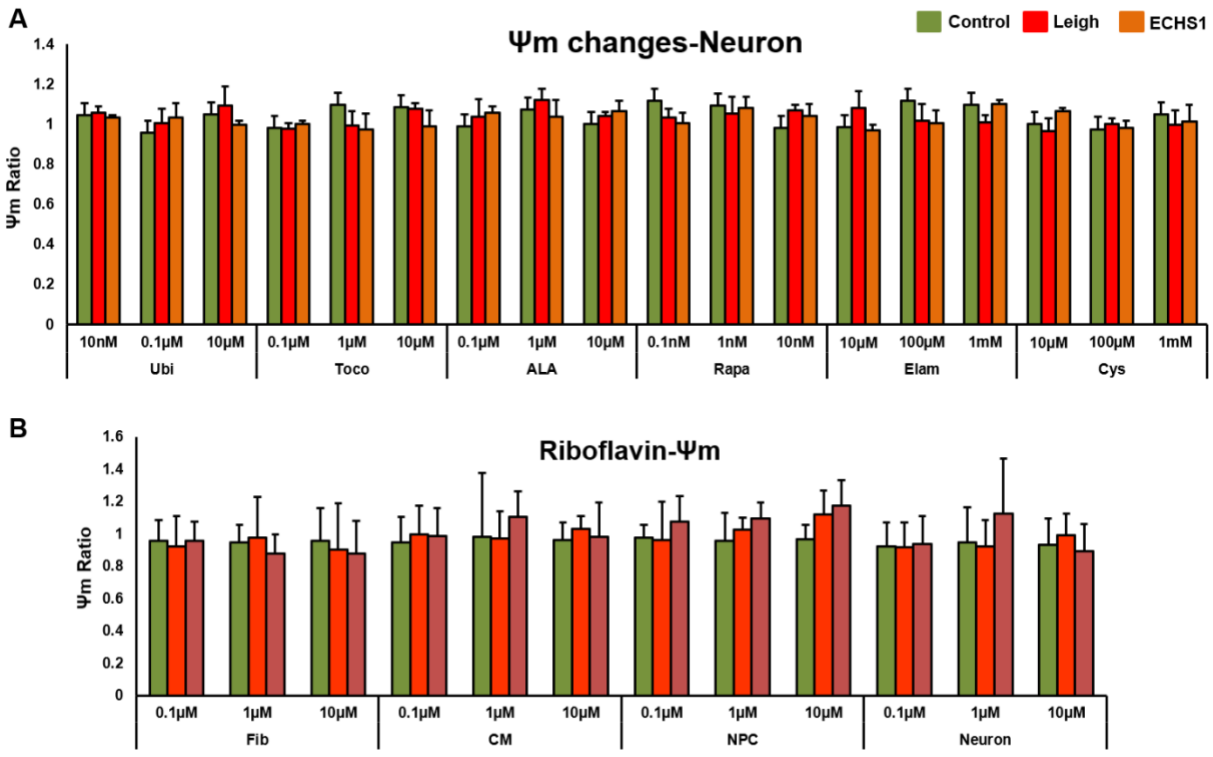

Supplementary Figure S13. Effect of drug panel on mitochondrial membrane potential: A Efficacy of a panel of six drugs on iPSC derived neurons from healthy control, LS and ECHS1 patients - Coenzyme Q10 (Ubiquinol: Ubi), Alpha-lipoic acid (ALA), Alpha-tocopherol (Toco), Cysteamine hydrochloride (Cys), Rapamycin (Rapa) and Elamipretide (Elam) was evaluated by determining the effects of individual drugs on mitochondrial membrane potential (Ψm) demonstrating no significant change throughout (n=3). **B** Riboflavin (Ribo) at different doses demonstrated no significant changes in the mitochondrial membrane potential in iPSC derived fibroblasts (Fibs), cardiomyocytes (CM), NPCs and neurons from healthy control, LS and ECHS1 patients (n=3). The "n" is representative of the biological replicates and were analyzed by one-way ANOVA. The data is representative of three independent experiments. Data is represented as mean ± SD; *$p<0.05$ in comparison to control.

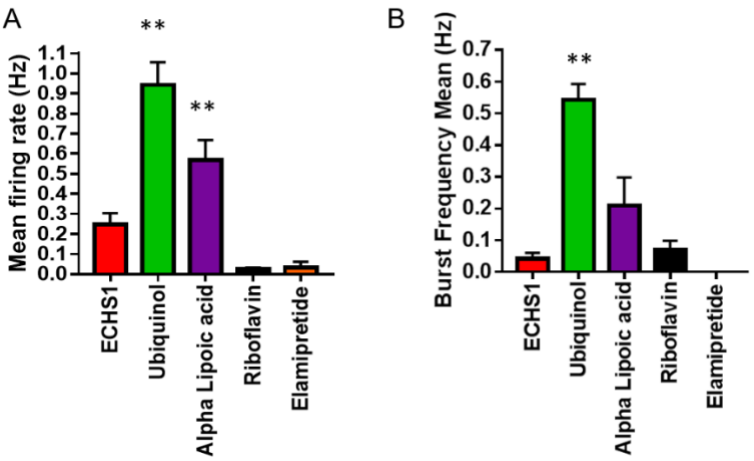

Supplementary Figure S14. MEA assessment of drug efficacy in ECHS1 iPSC derived neurons: A-B Histograms showing mean firing rate and burst frequency mean in neurons when treated with respective drugs (n=3). The "n" is representative of the biological replicates and were analyzed by one way ANOVA. The data is representative of three independent experiments. Data is represented as mean ± SEM; **p<0.01 in comparison to control (ECHS1).

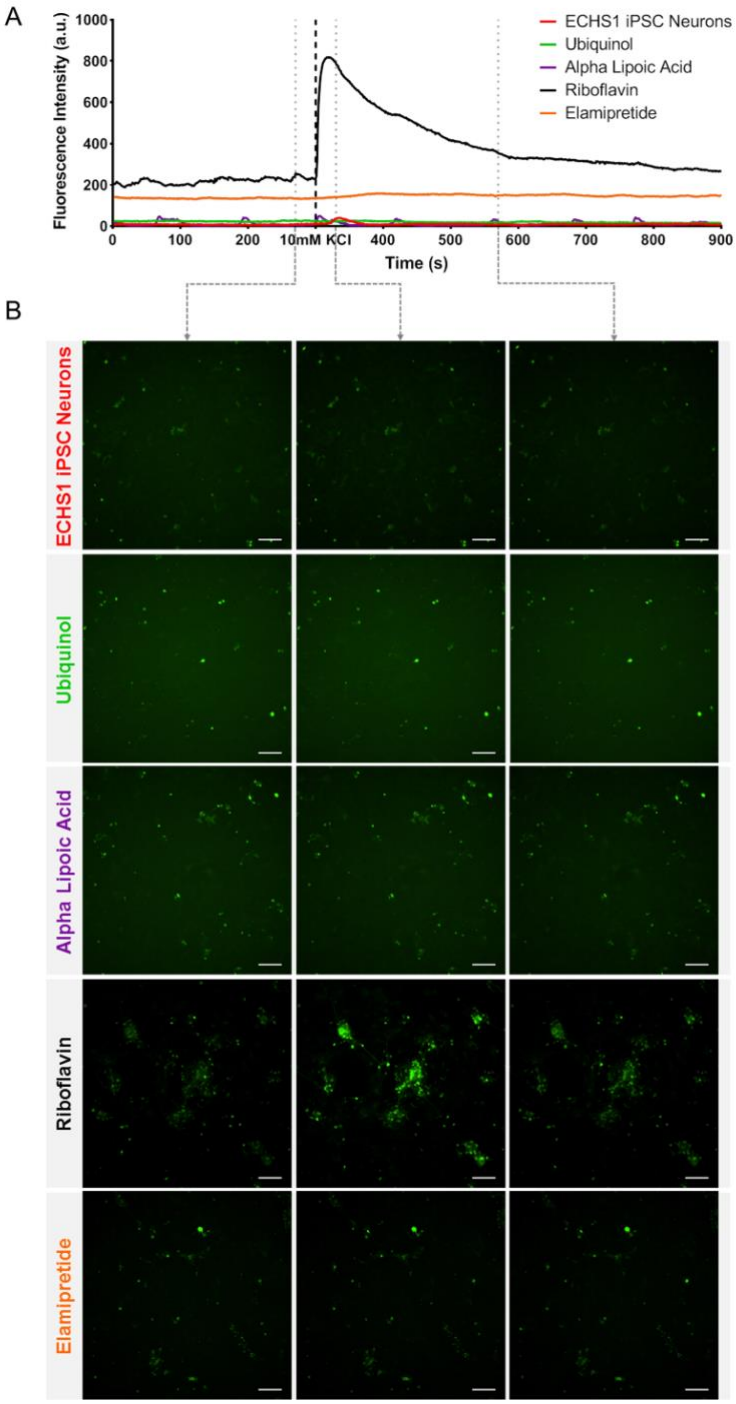

Supplementary Figure S15 Assessment of calcium handling in iPSC derived neurons: A Fluorescence intensity measuring Ca2+ traces for ECHS1 iPSC neurons at baseline and with drug administration during evoking of neurons with 10mM KCl (n=4). **B** Images depicting calcium response of groups at pre, just after evoking and during decay of calcium transits (n=4). The "n" is representative of the biological replicates. The scale bar is 100 µm.

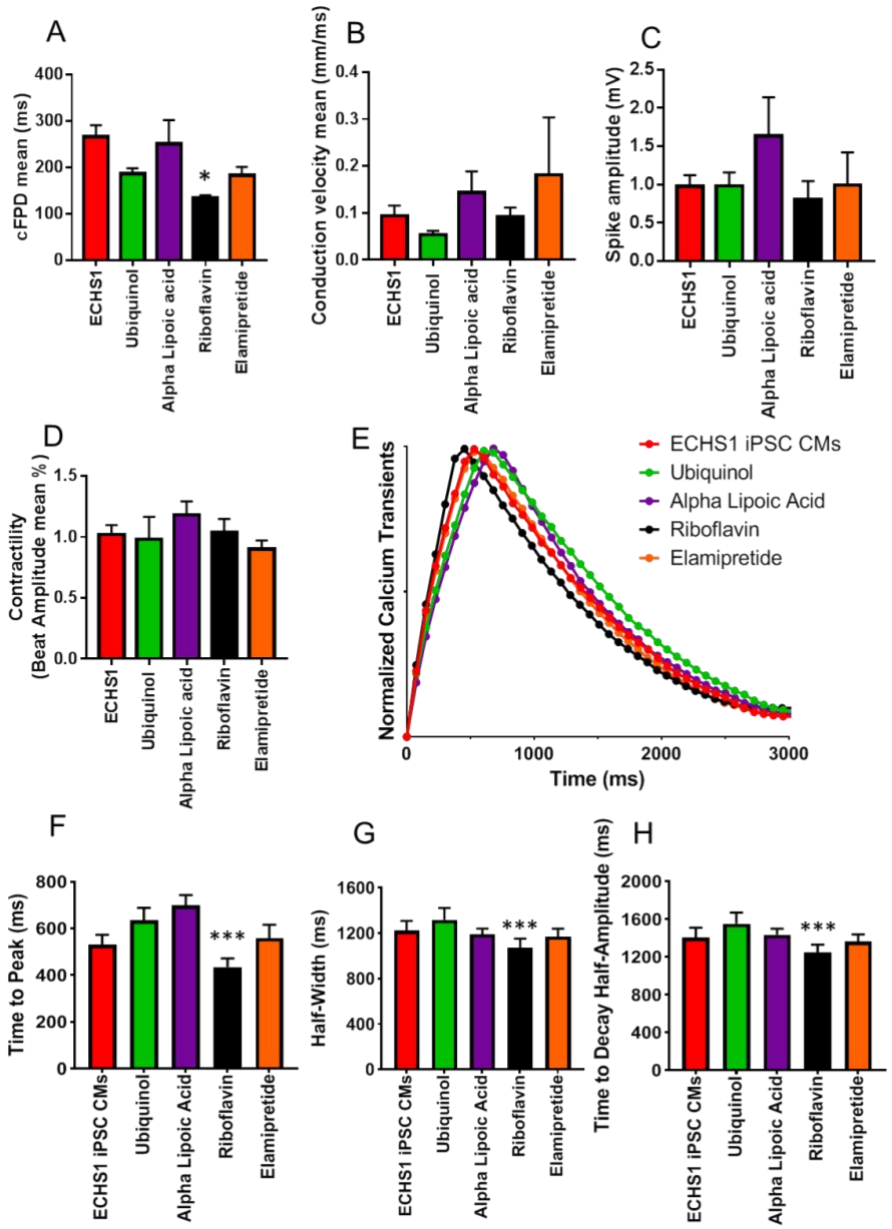

Supplementary Figure S16. MEA and calcium signaling assessment of drug efficacy in ECHS1 iPSC derived cardiomyocytes: A-D Corrected field potential delay, spike amplitude, conduction velocity and contractility after administration of respective drugs to ECHS1 iPSC-CMs (n=6). **E** Normalized action potential calcium transits comparing ECHS1 iPSC-CMs after administration of drugs (n=10). **F-H** Action potential wave properties of time to peak, half-width and time to decay half-amplitude in ECHS1 iPSC derived CMs after administration of respective drugs. Data were collected from 10 different regions of interest per loop and 80-130 beats were analyzed and plotted for every group of CMs. The "n" is representative of the biological replicates and were analyzed by one way ANOVA. The data are representative of three independent

experiments and presented as mean ± SEM; * p<0.05; **p<0.01 and ***p<0.001 in comparison to control (ECHS1).

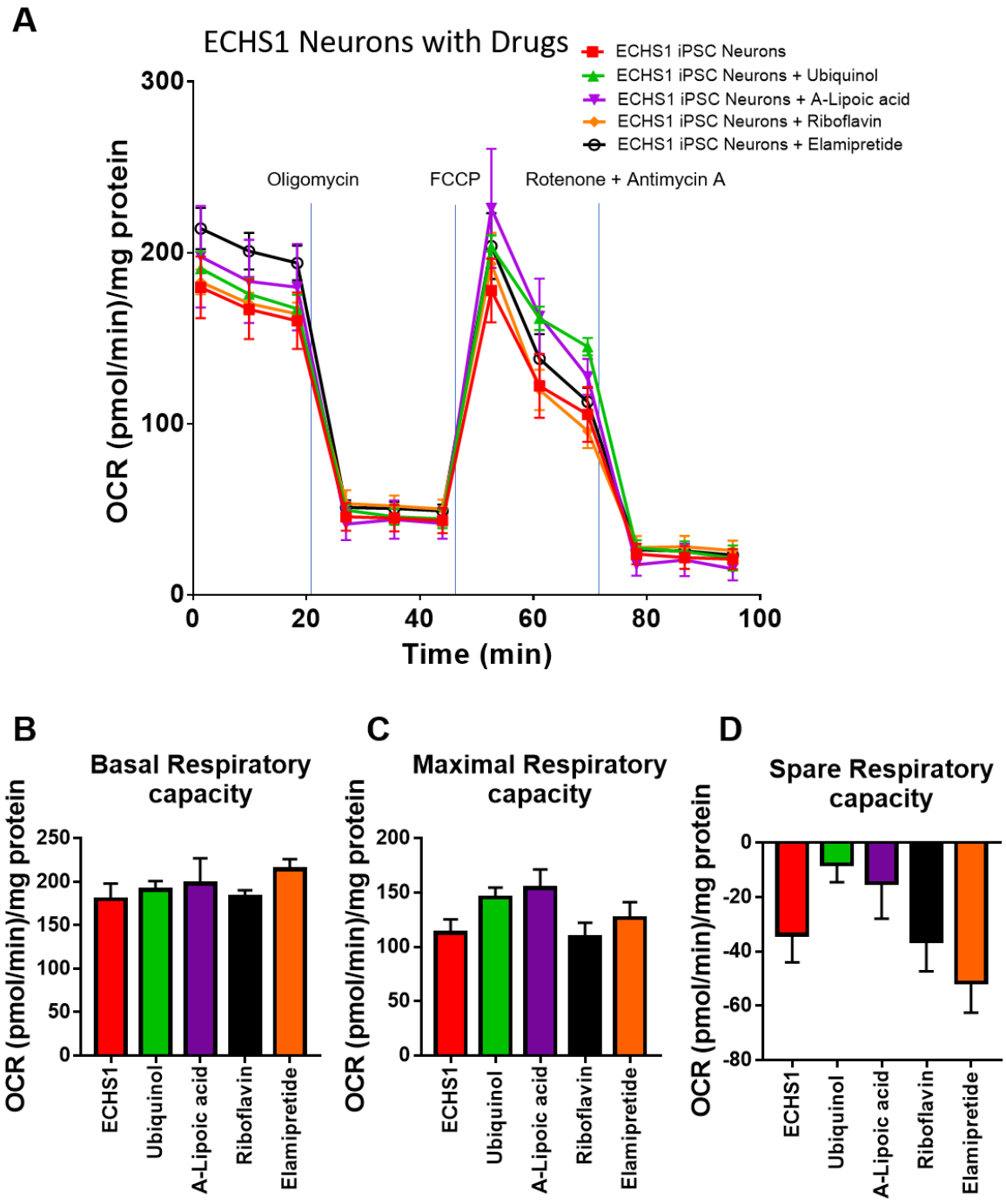

Supplementary Figure S17. Bioenergetics and mitochondrial respiration in ECHS1 iPSC derived neurons using SeaHorse XFe24 analyser: A Mitochondrial respiration; **B** Basal

respiration; **C** Maximal respiration; **D** Spare respiratory capacity. (n=3-4). The "n" is representative of the biological replicates and were analyzed by one-way ANOVA. The data are representative of three independent experiments and presented as mean ± SEM.

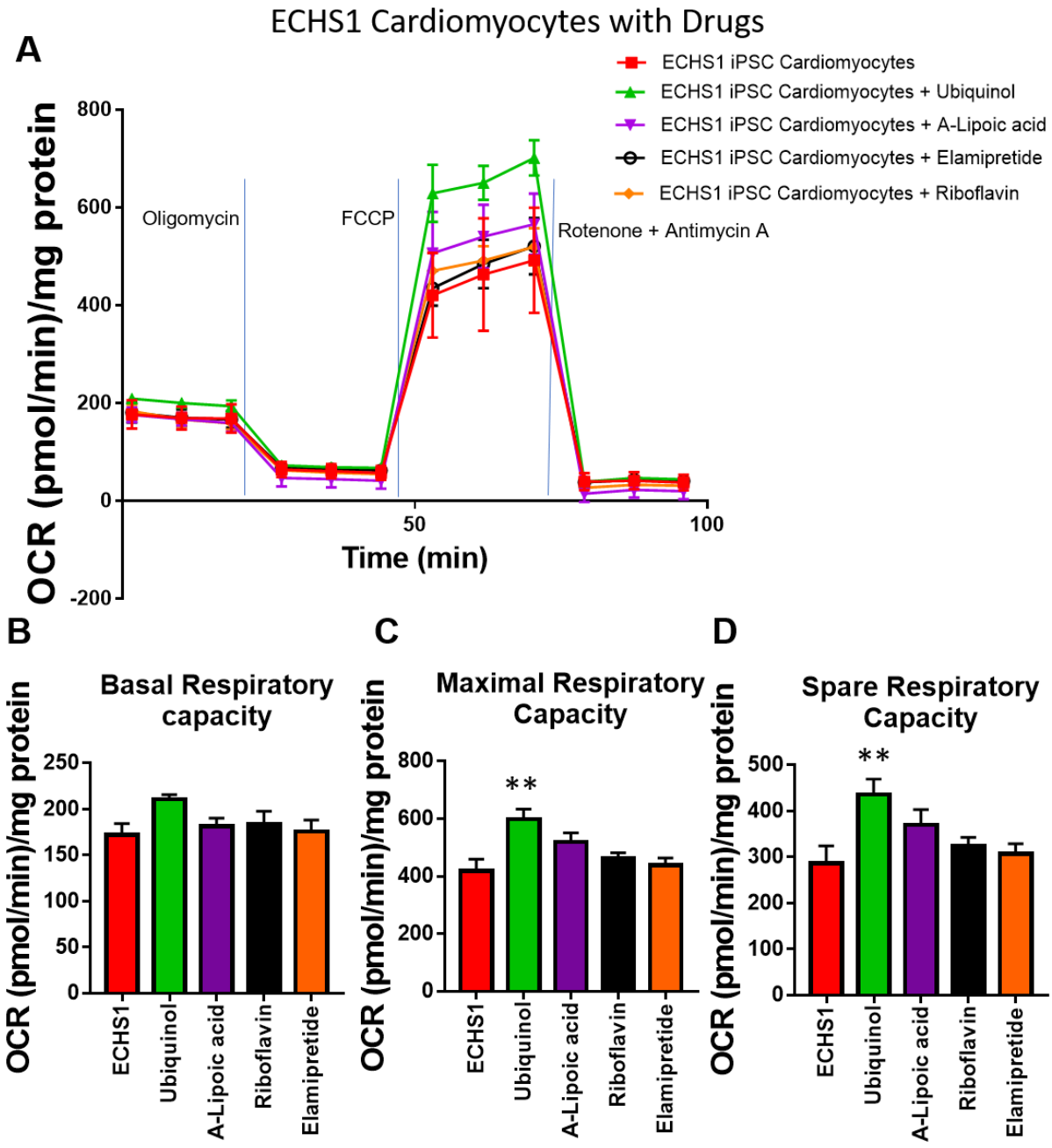

Supplementary Figure S18. Bioenergetics and mitochondrial respiration in ECHS1 iPSC derived cardiomyocytes using SeaHorse XFe24 analyser: A Mitochondrial respiration; **B** Basal respiration; **C-D** Maximal respiration and spare respiratory capacity, treatment with Ubi led to significant improvement. (n=3-4). The "n" is representative of the biological replicates and were

analyzed by one-way ANOVA. The data are representative of three independent experiments and presented as mean ± SEM; *p<0.05; **p<0.01 and ***p<0.001 in comparison to control.

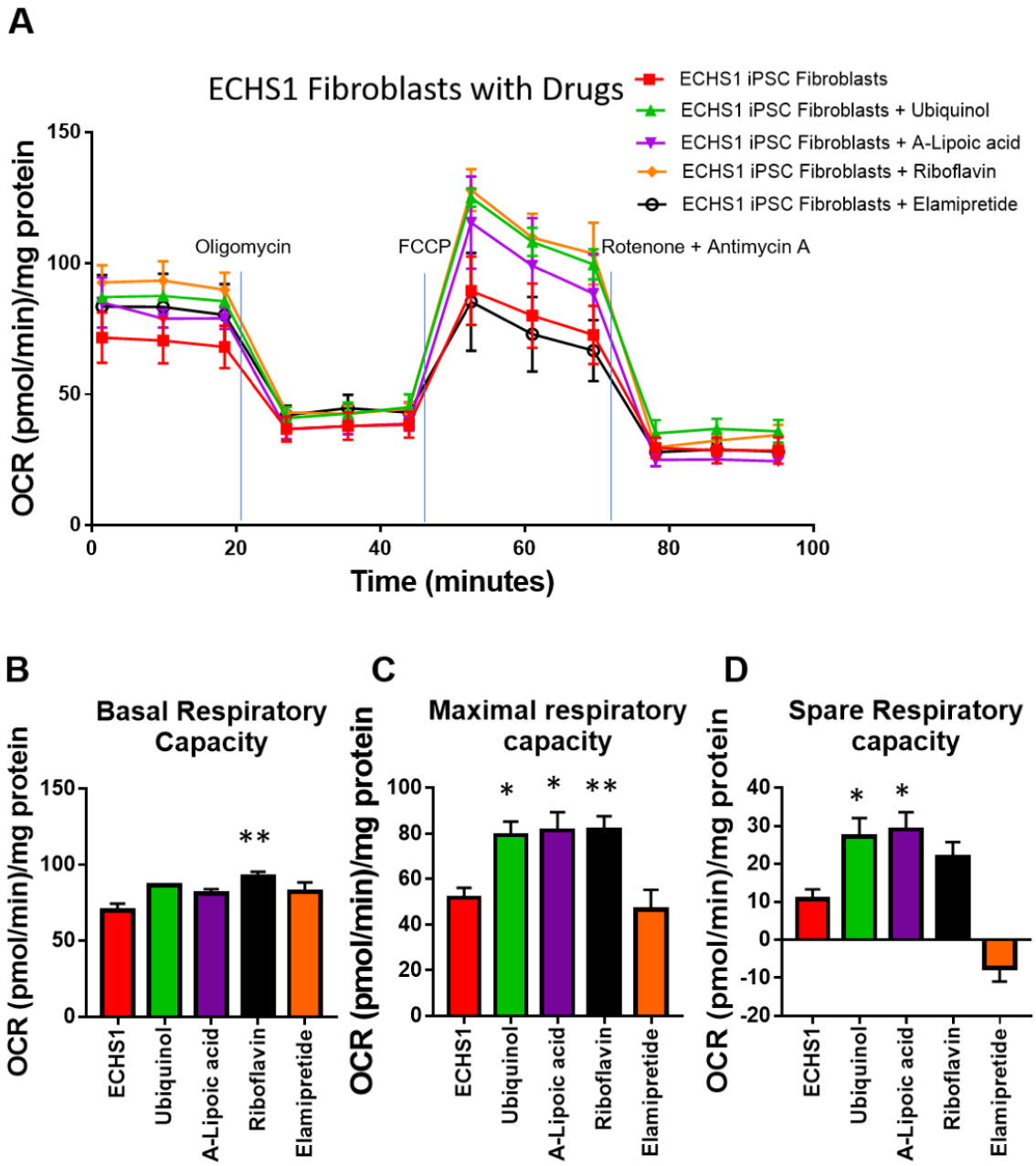

Supplementary Figure S19. Bioenergetics and mitochondrial respiration in ECHS1 iPSC derived fibroblasts using SeaHorse XFe24 analyser: **A** Mitochondrial respiration; **B** Basal respiration, treatment with Ribo led to significant improvement; **C** Maximal respiration, treatment with Ubi, ALA and Ribo led to significant improvement; **D** Spare respiratory capacity, treatment with Ubi and ALA led to significant improvement. (n=3-4). The "n" is representative of the biological replicates and were analyzed by one-way ANOVA. The data are representative of three

independent experiments and presented as mean ± SEM; *p<0.05; **p<0.01 and ***p<0.001 in comparison to control.

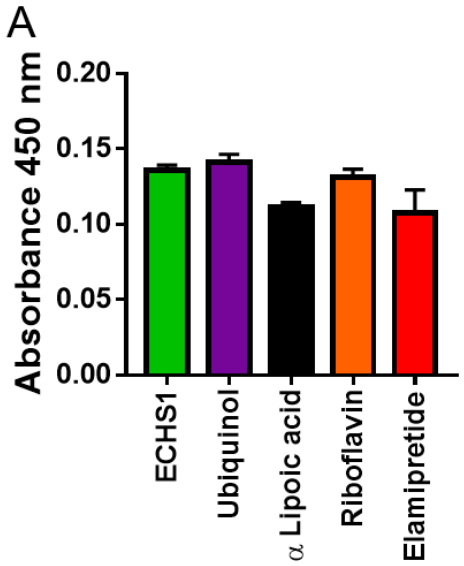

Supplementary Figure S20. Proliferation of ECHS1 iPSC derived fibroblasts in response to drug treatment: A Histograms showing fibroblast proliferation. Treatment with different drugs did not cause any significant change in the fibroblast proliferation. (n=5). The "n" is representative of the biological replicates and were analyzed by one-way ANOVA. Data are presented as mean ± SEM.

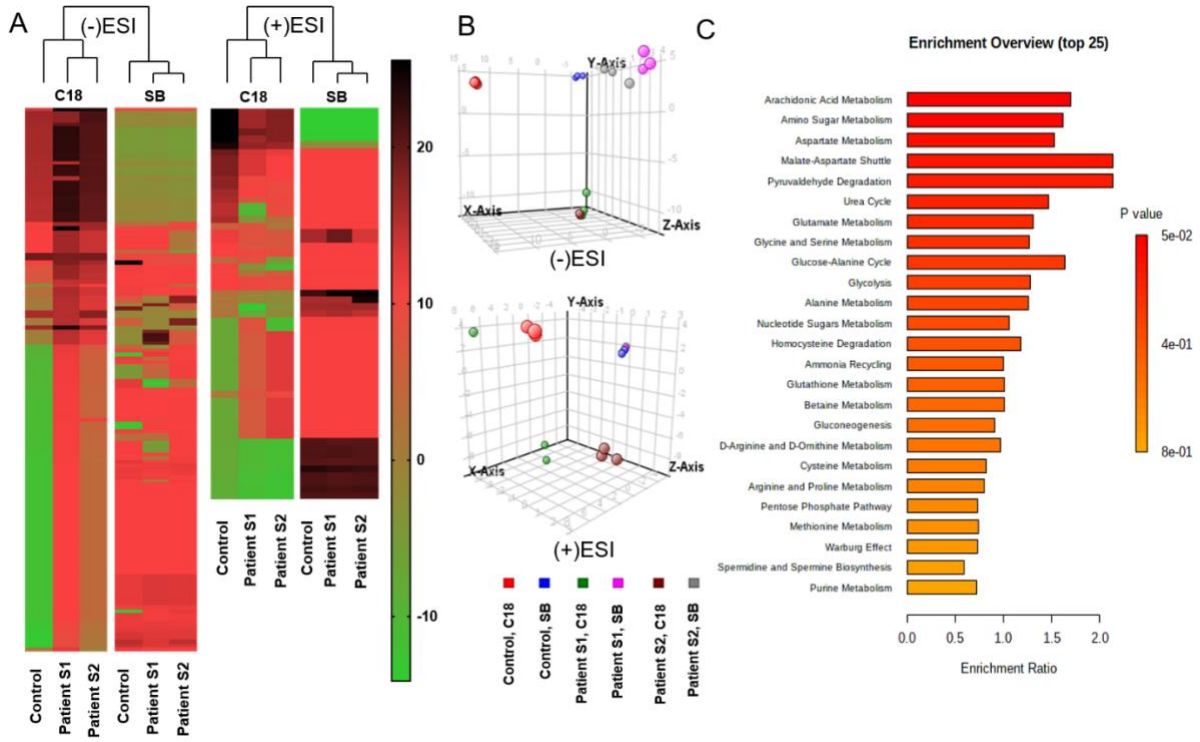

Supplementary Figure S21. Metabolomic analysis of ECHS1 patient before and after treatment: A Hierarchical clustering heat map representing a complete metabolomic profile of untreated (Patient Sample S1) and treated samples (Patient Sample S2) compared to control. Each row represents a metabolite (total 200 metabolites were detected). **B** Patrial least square discrimination (PLSD) of detected metabolites from two detection columns C18 and SB respectively on both positive and negative ESI settings to understand difference in individual metabolite population profiles for the respective samples. **C** Enrichment analysis using metaboanalyst^{TM} to understand the metabolic pathways affected in response to treatment with respect to the metabolomic profiles of the respective samples.

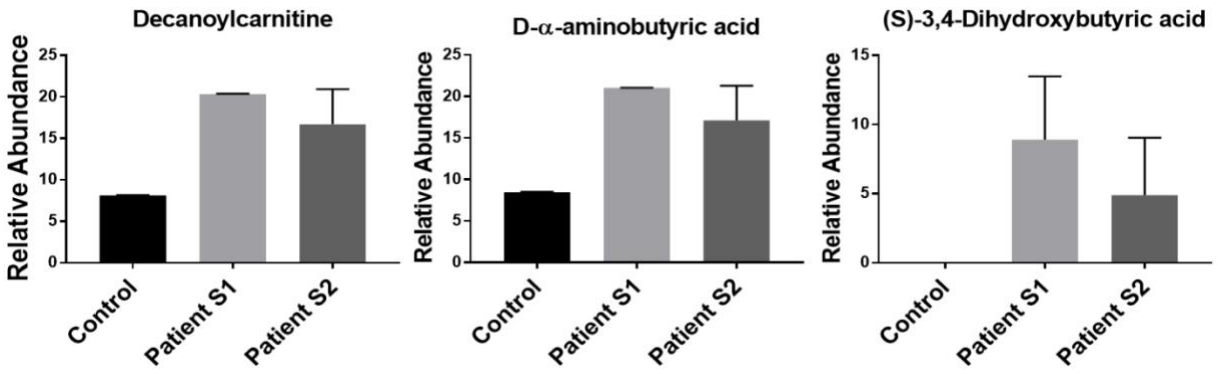

Supplementary Figure S22. Metabolic profile of ECHS1 patient before and after treatment. ECHS1 deficiency leads to accumulation of its substrates which can cause clinical complications in the patients. Histograms show a trend in reduction of accumulated metabolites such as decanoylcarnitine, aminobutyric acid and other butyric acid derivatives like 3,4-dihydroxybutanoic acid in Patient S2 (treated) when compared to Patient S1 (untreated). The graphs show relative metabolite abundance. The "n" is representative of technical replicates and were analyzed by two-way ANOVA. Data is represented as mean ± SEM.

Supplementary Table S1: Details of primers

Gene (Mutation)	**Forward**	**Reverse**
ECHS1_518	GATGTTCCCGGGCTCTTGTG	ACCCATACCTGCTTGCTTGG
ECHS1_849Del	AAGAAGGGATGACCGCGTTT	ACGCAGCAATTGGAGAGGAA
NDUFV1_529Dup	GGCAGCAAAGCAGCTTACTTAT	CACAGGACACAGTCTGACCC
NDUFV1_640	ATGAGGCAGGTCTGATTGGC	CACAGGACACAGTCTGACCC
Pluripotency Markers (Gene)	**Forward**	**Reverse**
Oct 3/4	AGCACTTCTGTCATGCTGGA	AGCACCTTCTATAAGCCAGCG
Sox 2	AAGGATAAGTACACGCTGCCC	GTTCATGTGCGCGTAACTGT
Nanog	CAATGGTGTGACGCAGAAGG	TGCACCAGGTCTGAGTGTTC
GAPDH (endogenous control)	ACAGTTGCCATGTAGACC	TTGAGCACAGGGTACTTTA